AFRL-SN-WP-TP-2004-100

ENHANCED PERFORMANCE OF BIPOLAR CASCADE LIGHT EMITTING DIODES BY DOPING THE ALUMINUM OXIDE APERTURES

William J. Siskaninetz

Electron Devices Branch (AFRL/SNDD)
Aerospace Components and Subsystems Division
Sensors Directorate
Air Force Research Laboratory, Air Force Materiel Command
Wright-Patterson Air Force Base, OH 45433-7320

J.E. Ehret
Materials and Manufacturing Directorate, AFRL/ML

J.A. Lott
Air Force Institute of Technology, AFIT

J.C. Griffith and T.R. Nelson, Jr.
Sensors Directorate, AFRL/SN

NOVEMBER 2004

Final Report for 01 July 2004 – 22 October 2004

Approved for public release; distribution is unlimited.

STINFO FINAL REPORT

SENSORS DIRECTORATE
AIR FORCE RESEARCH LABORATORY
AIR FORCE MATERIEL COMMAND
WRIGHT-PATTERSON AIR FORCE BASE, OH 45433-7320

NOTICE

/s/

WILLIAM J. SISKANINETZ
Electronics Engineer

/s/

KENICHI NAKANO
Chief, Electron Devices Branch

/s/

ROBERT T. KEMERLEY
Chief, Aerospace Components & Subsystems Division

REPORT DOCUMENTATION PAGE

Form Approved
OMB No. 0704-0188

1. REPORT DATE ***(DD-MM-YY)***
November 2004

2. REPORT TYPE
Journal Article Preprint

3. DATES COVERED ***(From - To)***
07/01/2004 – 10/22/2004

4. TITLE AND SUBTITLE
ENHANCED PERFORMANCE OF BIPOLAR CASCADE LIGHT EMITTING DIODES BY DOPING THE ALUMINUM OXIDE APERTURES

5a. CONTRACT NUMBER
In-House

5b. GRANT NUMBER

5c. PROGRAM ELEMENT NUMBER
69199F

6. AUTHOR(S)
William J. Siskaninetz (AFRL/SNDD)
J.E. Ehret (Materials and Manufacturing Directorate, AFRL/ML)
J.A. Lott (Air Force Institute of Technology, AFIT)
J.C. Griffith and T.R. Nelson, Jr. (Sensors Directorate, AFRL/SN)

5d. PROJECT NUMBER
N/A

5e. TASK NUMBER
N/A

5f. WORK UNIT NUMBER
N/A

7. PERFORMING ORGANIZATION NAME(S) AND ADDRESS(ES)

Electron Devices Branch (AFRL/SNDD)	AFRL/ML
Aerospace Components and Subsystems Division	
Sensors Directorate	AFRL/AFIT
Air Force Research Laboratory, Air Force Materiel Command	
Wright-Patterson Air Force Base, OH 45433-7320	AFRL/SN

8. PERFORMING ORGANIZATION REPORT NUMBER
AFRL-SN-WP-TP-2004-100

9. SPONSORING/MONITORING AGENCY NAME(S) AND ADDRESS(ES)
Sensors Directorate
Air Force Research Laboratory
Air Force Materiel Command
Wright-Patterson AFB, OH 45433-7320

10. SPONSORING/MONITORING AGENCY ACRONYM(S)
AFRL/SNDD

11. SPONSORING/MONITORING AGENCY REPORT NUMBER(S)
AFRL-SN-WP-TP-2004-100

12. DISTRIBUTION/AVAILABILITY STATEMENT
Approved for public release; distribution is unlimited.

13. SUPPLEMENTARY NOTES
To be published in *Applied Physics Letters*, Volume 86, 2005. This material is declared a work of the U.S. Government and is not subject to copyright protection in the United States.

14. ABSTRACT
Performance improvements in multiple-stage, single-cavity bipolar cascade light emitting diodes including reduced operating voltages, enhanced light generation, and reduced device heating are obtained by doping intracavity aluminum oxide apertures with silicon. This doping results in a reduced electron energy barrier and therefore a reduced series resistance which leads to better power and heating characteristics. Nearly 50% reductions in operating voltages, 200% increases in light power, and increased operating range are demonstrated. We discuss the direct implications of these results for the design of bipolar cascade vertical cavity surface emitting lasers.

15. SUBJECT TERMS
Optoelectronics, light emitting diodes, semiconductors

16. SECURITY CLASSIFICATION OF: a. REPORT	b. ABSTRACT	c. THIS PAGE	17. LIMITATION OF ABSTRACT:	18. NUMBER OF PAGES	19a. NAME OF RESPONSIBLE PERSON (Monitor)
Unclassified	Unclassified	Unclassified	SAR	14	William J. Siskaninetz
					19b. TELEPHONE NUMBER *(Include Area Code)* (937) 255-1874 x3515

Standard Form 298 (Rev. 8-98)
Prescribed by ANSI Std. Z39-18

Enhanced performance of bipolar cascade light emitting diodes by doping the aluminum oxide apertures

W. J. Siskaninetz

Sensors Directorate, Air Force Research Laboratory and

Department of Electrical and Computer Engineering,

Air Force Institute of Technology, Wright-Patterson AFB, Ohio 45433[*]

J. E. Ehret

Materials and Manufacturing Directorate,

Air Force Research Laboratory, Wright-Patterson AFB, Ohio 45433

J. A. Lott

Department of Electrical and Computer Engineering,

Air Force Institute of Technology, Wright-Patterson AFB, Ohio 45433[*]

J. C. Griffith and T. R. Nelson, Jr.

Sensors Directorate, Air Force Research Laboratory, Wright-Patterson AFB, Ohio 45433

Abstract

Performance improvements in multiple-stage, single-cavity bipolar cascade light emitting diodes including reduced operating voltages, enhanced light generation, and reduced device heating are obtained by doping intracavity aluminum oxide apertures with silicon. This doping results in a reduced electron energy barrier and therefore a reduced series resistance which leads to better power and heating characteristics. Nearly 50% reductions in operating voltages, 200% increases in light power, and increased operating range are demonstrated. We discuss the direct implications of these results for the design of bipolar cascade vertical cavity surface emitting lasers.

PACS numbers: 42.55.Px, 85.60.-q, 85.60.Jb

Single-cavity bipolar cascade (BC) vertical cavity surface emitting lasers (VCSELs) and light emitting diodes (LEDs) have shown great promise for increasing device slope and differential quantum efficiencies by epitaxially connecting in series active regions with reverse-biased tunnel junctions.[1,2] As with conventional p-i-n junction VCSELs, a common design feature of the BC variety is an aluminum oxide aperture (OA) or apertures that serve to funnel the injected current toward the center of the active region for better fundamental optical mode and gain overlap. While the active region and the tunnel junction have been studied extensively and optimized to improve device performance, the only considerations typically mentioned in the literature for the OA are optimum placement at nodes of the cavity resonance, material grading, tapering, and layer thickness. However, doping of the OA within the microcavity has not been discussed to the best of the authors' knowledge. This letter discusses how doping the OAs placed inside the microcavity of single- or multiple-stage BC LEDs significantly improves overall device performance by reducing the operating voltage, increasing the light power, and reducing junction heating.

Oxide aperture layers are routinely doped when they are located within a distributed Bragg reflector (DBR) stack in p-i-n junction VCSEL and single-stage BC VCSEL structures.[3,4] Generally, in single-cavity multiple-active-region BC structures undoped OAs are located within the mostly undoped (except for the degenerately doped tunnel junction layers) microcavity. The OA layers within the microcavity have been shown to reduce bistability effects due to current spreading between successive active regions.[5] Doping the microcavity OAs will increase losses due to scattering and free-carrier absorption, however, these losses will be shown to be much less than the gains achieved by doping the OAs.

The unbiased real-space energy band diagrams of doped ($N_d = 2 \times 10^{18}$ cm^{-3}) and undoped single-stage BC VCSELs with graded OA layers at thermal equilibrium are shown in Fig. 1. Doping the graded OA layer results in a significantly reduced conduction band barrier and thus more efficient transport of injected electrons to the quantum wells (left-to-right in Fig. 1). The smaller conduction band barrier also reduces junction heating by reducing the number of confined electrons trapped behind the barrier.

Our present investigation focuses on the OA layers and we have designed our experiment around a systematic series of BC LED structures, similar to that shown in the lower panel of Fig. 1. This structure allows us to disentangle the physics of the microcavity in BC devices from the additional complications that result from laser operation in a similar BC VCSEL structure.

To investigate the electrical, optical, and electroluminescent properties of the microcavities, BC LEDs were grown by molecular beam epitaxy in a Varian Gen II system. The BC LEDs were grown on n-type (100) GaAs substrates and consist of a microcavity designed to be in a BC VCSEL structure with one, two, three or more 2.5λ thick stages between 2000 Å thick Si doped ($N_d = 4 \times 10^{18}$ cm^{-3}) GaAs cladding layers. A single-stage device is shown schematically at the bottom of Fig. 1. Each 2.5λ thick stage consists of a graded OA located in the first node (left to right in Fig. 1), a triple quantum well active region located in the third antinode, and a tunnel junction located in the fifth node of the cavity resonance. Placing the OAs and tunnel junctions in the nodes minimizes losses and placing the quantum well in the antinode maximizes the gain achieved from the cavity. The graded OA consists of a 180 Å thick $Al_xGa_{1-x}As$ layer with x increasing from 0.1 to 0.9, a 300 Å thick $Al_{0.98}Ga_{0.02}As$ OA, and a 180 Å thick $Al_xGa_{1-x}As$ layer with x decreasing from 0.9 to 0.1. The graded OAs were Si doped with a doping concentration of $N_d \sim 2 \times 10^{18}$ cm^{-3}. The active region has three 80 Å thick $In_{0.20}Ga_{0.80}As$ quantum wells separated by 100 Å thick GaAs barriers. The GaAs tunnel junction (TJ) consists of a 200 Å thick ($N_a = 5 \times 10^{19}$ cm^{-3}) carbon doped p^{++} layer and a 200 Å thick Si -doped ($N_d \sim 2 \times 10^{19}$ cm^{-3}) n^{++} layer. Additional tunnel junction growth details appear elsewhere.[6]

The samples were processed into LEDs with square apertures and square annulus top metal contacts. The top and bottom (backside metal) ohmic contacts consist of a Ni:Ge:Au:Ni:Au metal layer profile that was annealed in a forming gas (95% Ar - 5% H_2) at 410°C for 15 seconds. Each device was dry etched using a BCl_3-Cl_2 recipe through the active region to form isolation mesas.

Voltage vs. current (V-I) and light power vs. current (L-I) characterization were performed using a probe station, a semiconductor parameter analyzer (SPA), and a 1 cm diameter silicon p-i-n photodetector positioned above the probes to maximize light collection across the entire current range. Since the photodetector was above the probes the collected light values are maximized relative values not absolute values. The electroluminescence (EL) characterization used the SPA as the constant current source and the output light was coupled into a silica multimode fiber (core diameter = 63 μm), aligned to maximize the collected light at 50 mA, and measured using an optical spectrum analyzer. Again, the power values are maximized relative values and not absolute values. Figure 2 shows the V-I measurements for 50μm $\times$ 50μm square 1-, 2-, and 3-stage BC LEDs with doped (dashed) and undoped (solid) OAs. Significant reductions in operating voltages are clearly observed for the doped OA devices, compared to the undoped OA devices. We also see nearly uniform voltage steps in going from one to three BC stages. This indicates that the 1 to 3 combinations of OA and TJ are the dominant series resistances as we would expect for good

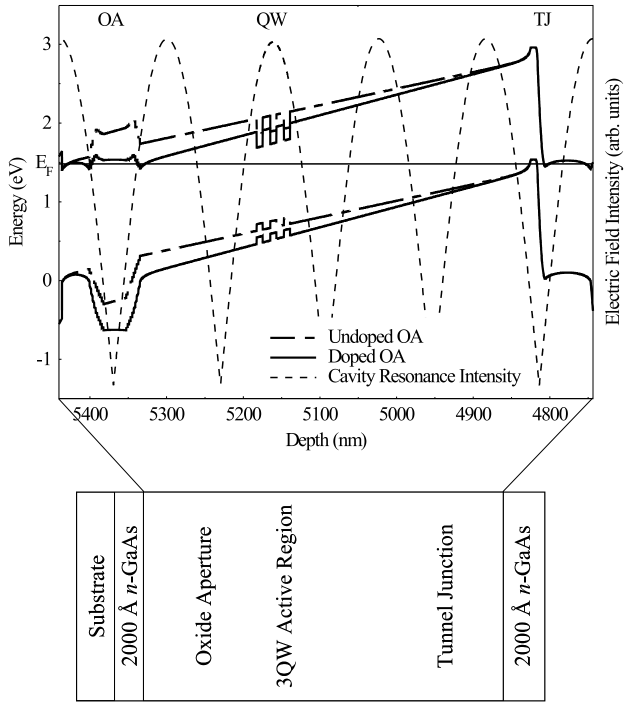

FIG. 1: Calculated electric-field intensity (dashed lines) and real-space energy band diagrams of a single-stage BC VCSEL with undoped (semi-dashed lines) and doped ($N_d = 2 \times 10^{18}$ cm^{-3}) oxide apertures (solid lines) in and around the microcavity active region (the top and bottom DBRs are not shown). Also shown is a schematic diagram of a single-stage BC LED device with the BC VCSEL microcavity.

devices. The doped OA devices demonstrate nearly a 50% reduction in operating voltage when compared to undoped OA devices with the same number of stages. The scaling between successive stages is very uniform with about 1.5 V per stage voltage for the doped graded OA structures and about 2.7 V per stage voltage for the undoped OA structures.

Figure 3 shows the L-I measurements for the same 50μm $\times$ 50μm square 1-, 2-, and 3-stage BC LEDs with doped (dashed) and undoped (solid) OAs. Significant increases in light power are clearly observed with OA doping. The 2- and 3-stage devices with doped OAs have a nearly a 200% improvement in light power at 30 mA. Saturation effects are also evident in the undoped and 3-stage doped OA devices due most likely to junction heating. The L-I curves of the undoped OA devices roll over at smaller current densities due to increased junction heating as a result of the larger electron injection barrier. It is also evident that the 3-stage doped OA device is showing evidence of saturation due to junction heating implying that the power output of a BC LED with a 4th active region stage would further suffer from junction heating and thus would less efficient

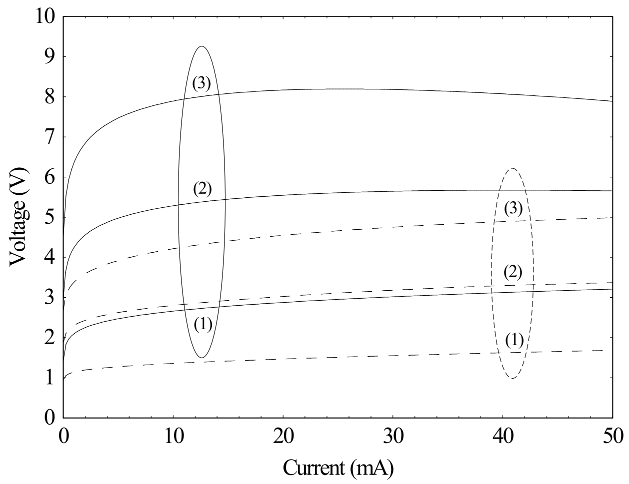

FIG. 2: Measured voltage vs. current for $50\mu\text{m} \times 50\mu\text{m}$ BC LEDs with doped (dashed lines) and undoped (solid lines) OAs. The number in parentheses indicates number of active region stages.

overall. This has been verified by growing and investigating a doped 4-stage BC LED and the L-I is less than the 3-stage device. Table I indicates the current where the onset of thermal saturation effects occurs for each device.

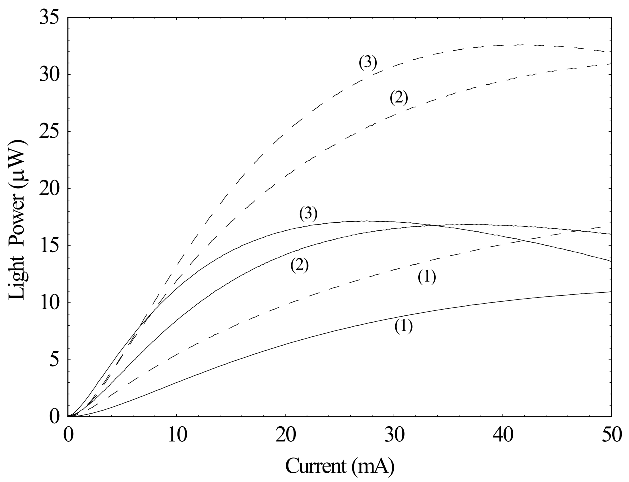

FIG. 3: Measured light output power vs. current for $50\mu\text{m} \times 50\mu\text{m}$ BC LEDs with doped (dashed lines) and undoped (solid lines) OAs. The number in parentheses indicates number of active region stages.

Figure 4 shows the EL spectra at 50 mA for the same series of BC LEDs. The undoped OA samples exhibit significantly lower quantum well luminescence and have pronounced red shifts in both the quantum well and GaAs emissions as compared to the doped OA samples. These differences are attributed to greater device heating in the undoped OA samples. These shifts are tabulated in detail in Table I. The quantum well and GaAs peak wavelengths indicate larger red shifts per stage for the undoped OA structures (∼10-20 nm) as compared to the doped OA structures (∼10-12 nm).

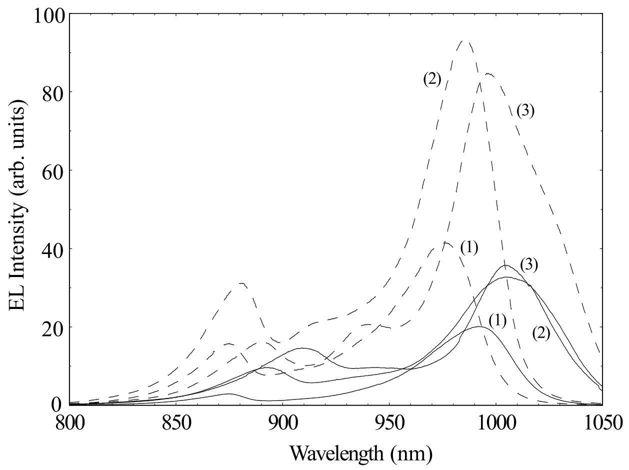

FIG. 4: Measured EL spectra at 50 mA for 50μm × 50μm BC LEDs with doped (dashed lines) and undoped (solid lines) OAs. The number in parentheses indicates number of active region stages. The EL intensity is the maximum relative power collected by a silica multimode fiber and not an absolute power measurement.

TABLE I: Current at thermal rollover and EL peak wavelengths at 50 mA for doped and undoped 50μm × 50μm square oxide aperture (OA) devices at room temperature.

Structure	Current at Light Peak (mA)	GaAs Peak (nm)	QW Peak (nm)
1-Stage Doped OA	$\gg$50	874.7	976.0
2-Stage Doped OA	$>$50	880.6	985.0
3-Stage Doped OA	39.4	890.9	996.5
1-Stage Undoped OA	∼50	874.9	992.7
2-Stage Undoped OA	35.6	893.0	1004.8
3-Stage Undoped OA	26.3	909.7	1004.8

This research shows that doping the graded intracavity OAs of BC LEDs significantly improves device performance by reducing the applied voltage, increasing optical recombination, reducing the red shift due to device heating, and increasing the saturation current where thermal rollover becomes evident. This doped OA technique has immediate applications for BC VCSEL designs.

By placing doped OAs in the microcavities of VCSELs, as shown in the top panel of Fig. 1, a laser structure with significantly improved power/performance characteristics should be achieved. For VCSEL designs with intracavity contacts, the smaller series resistance should result in higher modulation frequencies in addition to the improved light output vs. power characteristics seen in the LED structures.

The authors would like to thank J. Breedlove, P. Cassity, L. Callahan, and D. Beasley of Wyle Laboratories and W. Rice of Wright State University for their technical support. Support from the Air Force Office of Scientific Research via LRIR 2305DW01 is gratefully acknowledged. WJS also recognizes the funding support of the Dayton Area Graduate Studies Institute.

---

[*] Electronic mail: `william.siskaninetz@wpafb.af.mil`

[1] T. Knödl, G. Golling, A. Straub, R. Jager, R. Michalzik, and K. Ebeling, IEEE J. Select. Topics Quantum Electron. **9**, 1406 (2003).

[2] J.K. Kim, E. Hall, O. Sjlund, G. Aleneau, and L. A. Coldren, Electron. Lett. **35**, 1084 (1999).

[3] K.D. Choquette, J.F. Klem, A.J. Fischer, O. Blum, A.A. Allerman, I.J. Fritz, S.R. Kurtz, W.G. Breiland, R. Sieg, K.M. Geib, J.W. Scott, and R.L. Naone, Electron. Lett. **36**, 1388 (2000).

[4] J.J. Wierer, D.A. Kellogg, and N. Holonyak, Jr., Appl. Phys. Lett. **74**, 926 (1999).

[5] T. Knödl, R. Michalzik, M. Golling, and K.J. Ebeling, Appl. Phys. Lett. **81**, 583 (2002).

[6] W.J. Siskaninetz, J.E. Ehret, T.N. Dang, J.E. Van Nostrand, J.A. Lott, and T.R. Nelson, Electron. Lett. **38**, 1259 (2002).